Solid-State Characterization of PEG 4000/ Monoolein Mixtures

Denny Mahlin,† Annika Ridell,*,† Göran Frenning,† and Sven Engström‡

Department of Pharmacy, Uppsala University, Uppsala Biomedical Center, Box 580, SE-751 23 Uppsala, Sweden, and Department of Materials and Surface Chemistry, Chalmers University of Technology, SE-412 96 Göteborg, Sweden

Received September 24, 2003
Revised Manuscript Received January 30, 2004

Introduction

Solid-state dispersions have received great scientific and technological interest in the pharmaceutical field.[1−4] One reason is the possibility to facilitate dissolution of poorly soluble drugs by predispersing them in a hydrophilic matrix. Solid poly(ethylene glycol)s (PEGs) dissolve easily in water and are used as carriers for dispersed drugs.[3,5] One example is the dispersion of the drug griseofulvin in PEG 6000.[6,7]

In this work we investigate the solid-state behavior of a mixture of a lipophilic component, the polar lipid monoolein (1-glyceryl monooleate, MO), and PEG of molecular weight 4000 (PEG 4000) with the objective of creating a matrix of increased lipophilicity. MO is orally nontoxic and biodegradable.[8] It has a fascinating phase behavior in water, forming a cubic phase which has been utilized in several areas of biotechnology, such as drug delivery[9,10] and membrane protein crystallization.[11]

The phase behavior of the three-component system, water−MO−PEG, was recently characterized.[12] The interaction between various surfactants and PEG in the solid state has been investigated,[7,13,14] as has the melting behavior of mixtures of PEGs and selected fatty acids.[15] Even though several recent studies have analyzed the solid-state structure of semicrystalline polymers, including the influence of addition of a second component,[16−19] a solid dispersion of a lipid in a solid polymer matrix has, to the best of our knowledge, not been extensively characterized.

In this article we used differential scanning calorimetry (DSC), together with small- and wide-angle X-ray scattering (SAXS and WAXS), to investigate solid-state mixtures of PEG and MO prepared by comelting the components.

Experimental Methods

Materials. PEG 4000 (mol wt 3500−4500, Merck, Germany) was used as received. MO of technical grade (RYLO MG 19 Pharma, lot no. 2119/83) was a gift from Danisco Cultor (Denmark).

Sample Preparation. PEG and MO were weighed and mixed in glass ampules and melted at 70 °C for 20 min, during intermittent vortexing. The heated, visually homogeneous and crystal-clear mixtures all solidified in less than 1 day at 25 °C.

DSC. DSC was performed in an N_2 atmosphere using a Seiko DSC 220 differential scanning calorimeter SSC/5200H (Seiko, Japan). The analysis of each sample (3−4 mg) was started after 5 min at 0 °C by heating at a rate of 5 °C/min until 150 °C was reached, and the sample was completely melted. The heat of fusion per gram sample (ΔH_m) was determined by measuring the melting peak area for each component. The relative PEG bulk crystallinity, α, was determined from

$$\alpha = \frac{\Delta H_m^{\mathrm{PEG,sample}}}{\Delta H_m^{\mathrm{PEG,pure}} X_{\mathrm{PEG}}} \quad (1)$$

where X_{PEG} is the PEG weight fraction. The weight fraction of MO phase was determined from

$$X_{\mathrm{MOphase}} = \frac{\Delta H_m^{\mathrm{MO,sample}}}{\Delta H_m^{\mathrm{MO,pure}}} \quad (2)$$

SAXS. SAXS experiments were performed on a modified Kratky camera with a linear position-sensitive detector (MBraun, Graz, Austria) using Cu Kα X-rays (wavelength 1.542 Å) provided by an X-ray generator operated at 50 kV and 40 mA (Philips, PW 1830/40, The Netherlands). A tungsten beam stop was used. The samples were placed between mica windows, and the temperature was controlled by a Peltier element at 25 °C (accuracy 0.1 °C). Each measurement was performed for 10 h in a vacuum.

The one-dimensional correlation function[20] $\gamma_1(x)$ was calculated by using

$$\gamma_1(x) = \frac{1}{2\pi Q}\int_0^\infty q[I(q) - I_b][J_0(qx) - qxJ_1(qx)]\,\mathrm{d}q \quad (3)$$

which is appropriate for intensity data collected by a slit of infinite length.[21] Here $q \equiv (4\pi/\lambda)\sin(\theta)$, 2θ being the scattering angle and λ the wavelength, $I(q)$ is the slit-smeared intensity, I_b is the background, and J_0 and J_1 are Bessel functions. The normalization by the scattering invariant

$$Q \equiv \frac{1}{2\pi}\int_0^\infty q[I(q) - I_b]\,\mathrm{d}q \quad (4)$$

ensures that $\gamma_1(0) = 1$. When evaluating the integral in eq 3, the experimental intensity was extrapolated to $q = \infty$ by using the Porod−Ruland model[22]

$$I(q) - I_b = \frac{K}{q^3}\left[1 - 2\sigma^2q^2\,\mathrm{erfc}(\sigma q) + \frac{2\sigma q\exp(-\sigma^2q^2)}{\sqrt{\pi}}\right] \quad (5)$$

and to $q = 0$ by using the Debye−Bueche model[23,24]

$$I(q) - I_b = \frac{I_0}{(1 + \xi^2q^2)^2} \quad (6)$$

In these expressions K, σ, I_0, and ξ are constants, and erfc is the complementary error function. The parameters I_b, K, and σ were determined by fitting eq 5 to $I(q)$ for $q > 0.08$ Å^{-1}, while I_0 and ξ were determined from a fit of eq 6 to $I(q)$ for $q < 0.027$ Å^{-1}. The integral in eq 3 was evaluated by using the FORTRAN routine D01GAF provided by the Numerical Algorithms Group (NAG Ltd., UK). The Bessel functions J_0 and J_1 were evaluated by using the NAG routines S17AEF and S17AFF, respectively.

WAXS. WAXS experiments were performed on a Diffractor D5000 (Siemens, Germany) equipped with a scintillation detector using Cu Kα radiation, 45 kV and 40 mA. Bragg−Brentano focusing geometry was used, and the samples were scanned in steps of 0.02° from 17 to 25° (2θ). The detection step time was 60 s. This procedure was performed twice on the same sample to ensure that the X-rays did not influence the sample.

Results and Discussion

DSC. Thermograms (not shown) for freshly prepared PEG samples displayed, in agreement with earlier

† Uppsala University.
‡ Chalmers University of Technology.
* Corresponding author: tel +46 18 471 4361; fax +46 18 471 4377; e-mail Annika.Ridell@farmaci.uu.se.

10.1021/ma0354344 CCC: $27.50
Published on Web 03/12/2004

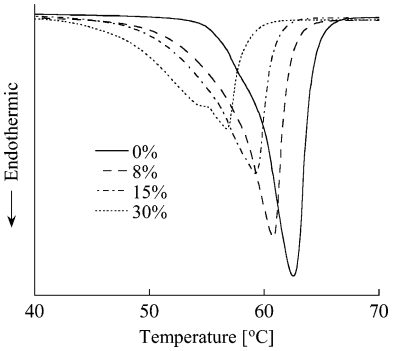

Figure 1. Thermograms of samples containing mixtures of PEG 4000 and MO. The amount of MO is indicated. Only the peak for PEG 4000 is shown (for the MO peak see Figure 2).

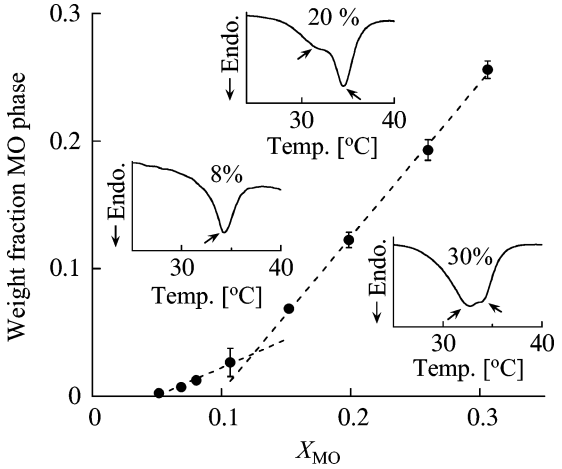

Figure 2. Amount of detected MO phase per gram of sample as a function of the total amount of MO in the samples. The DSC thermograms of the MO peak for samples containing 8, 20, and 30% MO are inserted. Arrows indicate melting peaks for the two forms of MO. Each point represents the mean ± the standard deviation, of five experiments.

reports,[25] a double melting peak, with melting temperatures at 55.5 and 61.0 °C for the once- and nonfolded PEG (the stable form), respectively. After approximately 1 month of storage the smaller lower temperature peak disappeared.

Representative thermograms obtained for solid samples of pure PEG and mixtures of PEG/MO after 2 months storage at room temperature are shown in Figure 1. For pure PEG, ΔH_m was 208.6 J/g, which is slightly higher than values previously reported in the literature (196.4−205 J/g),[26−30] indicating that the pure PEG was highly crystalline. In samples with MO, PEG showed a relative crystallinity, α, of 98 ± 1%, and no glass transition temperature (T_g) was detected in the interval −150−20 °C, indicating a low amorphous content.

For samples containing 5% MO or more, a second melting endotherm was detected and assumed to originate from the formation of a pure MO phase. Utilizing eq 2, the weight fraction pure MO phase in the mixtures vs total weight fraction MO was calculated (see Figure 2). For low MO contents (5−10%), Figure 2 reveals that the amount of MO phase increases linearly with the slope 0.44 ± 0.06, whereas the slope for higher MO contents (>15%) was 1.21 ± 0.02. These slopes indicate that the intercalated amount of MO increases with increasing MO content up to 15%, whereas it remains more or less constant at higher contents. The maximum amount of MO dissolved in PEG was 8.5% at the total composition of 15% MO.

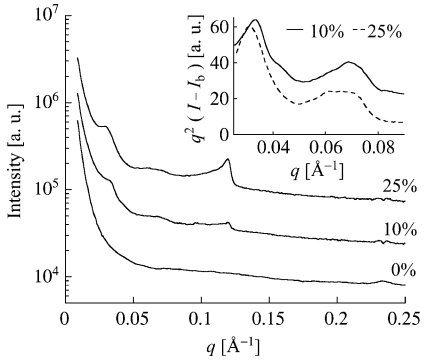

Figure 3. Uncorrected SAXS intensity data obtained for samples of three different compositions. The inset shows the Lorentz-corrected intensity for the MO-containing samples. The amount of MO is indicated in the figure.

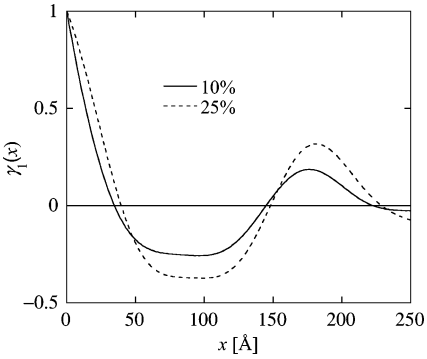

Figure 4. One-dimensional correlation function for samples of two different compositions, as indicated in the figure.

The insets in Figure 2 show the double melting peak for MO present at 15−30% MO. The positions of the two peaks coincide with those obtained for the β (35 °C) and β′ (32 °C) polymorphs of MO,[31−33] and the peak area of the β form increases with increasing MO content in this region.

SAXS. The uncorrected SAXS spectra, shown in Figure 3, exhibit for MO-containing samples two sets of peaks: one at low q values (0.02−0.08 Å^{-1}) and another at q = 0.12 Å^{-1}. The first set of peaks, seen more clearly in the Lorentz-corrected spectrum shown in the inset of Figure 3, was observed for samples containing 2.5% MO or more and is attributed to the packing of the amorphous and crystalline PEG domains (see below). For samples containing 10% MO or more, a peak at q = 0.12 Å^{-1} was observed, and its intensity increased with increasing MO content. It is evident that this peak appears as a consequence of the formation of a separate MO phase, and since its position remains the same, there is no shift in the lipid bilayer thickness as the MO concentration is increased. This indicates that no PEG is incorporated into the MO phase.

To analyze the PEG structure further, the one-dimensional correlation function was calculated (shown in Figure 4). To minimize interference with the MO peak, intensity values for $q \leq 0.09$ Å^{-1} were used in this calculation. The appearance of the correlation function is consistent with the assumption that PEG exhibits a lamellar structure; i.e., the morphology is characterized by lamellae of alternating crystalline and amorphous phases.[34] The long period (most probable repeat), L, of the lamellar stacks was determined from the first maximum in the correlation function. The thickness of the crystalline (l_c) and amorphous (l_a) regions within the

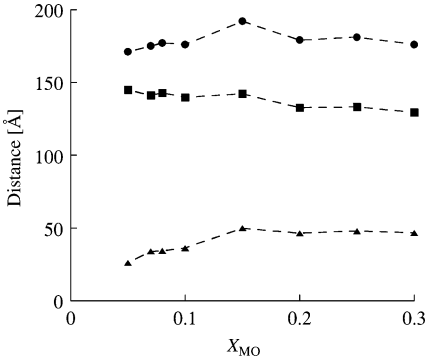

Figure 5. Results from the SAXS analysis. Circles correspond to L, long period, squares to l_c, crystalline layer thickness, and triangles to l_a, amorphous layer thickness.

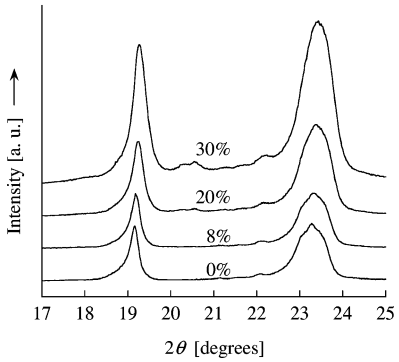

Figure 6. WAXS results for samples containing different amounts of MO, as indicated in the figure.

lamellar structure was determined according to the method described by Santa Cruz et al.[35] The crystalline thickness was identified by comparison with DSC data and the known thickness of a nonfolded and a once-folded PEG molecule. The calculated values of L, l_c, and l_a are shown in Figure 5.

The distance l_c shows a modest decrease from 145 to 129 Å when the MO content increases. Since a once-folded PEG 4000 has a typical length of 123 Å,[25] this result indicates that folded PEG molecules constitute the crystalline lamellae. The shorter distance l_a increases when the amount of MO increases from 5 to 15% and is approximately 50 Å for higher MO contents. Together with DSC data, this finding shows that MO is intercalated into the amorphous regions. The long period, being the sum of l_c and l_a, first increases with increasing MO contents and then decreases slightly.

WAXS. Figure 6 shows the WAXS diffractograms of the PEG/MO mixtures. The two intense peaks, originating from PEG, were centered at 19.2° and 23.3° (2θ) for all mixtures, showing that the helix crystallization of PEG is unaltered when MO is added. The β-polymorph of MO has one large peak at 19.3° and two others at 20.3° and 20.5°, whereas the β'-polymorph, according to the literature,[32,33] has one smaller peak at 21.15° and a larger one at 23.4°. The two separate peaks at 20.3° and 20.5° were not detectable in the 8% MO sample but were found with low intensities in the 20% and 30% samples. Since the PEG and MO peaks overlap, no quantitative analysis could be done to verify the different polymorphs of MO.

Summary and Conclusions

Solid-state mixtures of PEG 4000 and MO were characterized utilizing DSC, SAXS, and WAXS. The mixtures were found to exhibit lamellar structures. MO partially induced a stabilization of the folded form of PEG and was intercalated into its amorphous lamellae. A solid solution of MO in PEG exists at up to 5% MO before a separate MO phase forms, as detected by DSC. Above 10% a second phase of MO occurs, as detected by SAXS, DSC, and WAXS.

Acknowledgment. Nils-Olof Ersson, Department of Materials Chemistry, Uppsala University, is gratefully acknowledged for technical assistance.

References and Notes

(1) Serajuddin, A. T. M. *J. Pharm. Sci.* **1999**, *88*, 1058−1066.
(2) Pedersen, G. P.; Fäldt, P.; Bergenståhl, B.; Kristensen, H. G. *Int. J. Pharm.* **1998**, *171*, 257−270.
(3) Leuner, C.; Dressman, J. *Eur. J. Pharm. Biopharm.* **2000**, *50*, 47−60.
(4) Corveleyn, S.; Remon, J. P. *Int. J. Pharm.* **1998**, *166*, 65−74.
(5) Craig, D. Q. M. *Drug Dev. Ind. Pharm.* **1990**, *16*, 2501−2526.
(6) Sjökvist, E.; Nyström, C.; Aldén, M. *Int. J. Pharm.* **1989**, *54*, 161−170.
(7) Wulff, M.; Aldén, M. *Thermochim. Acta* **1995**, *256*, 151−165.
(8) Wade, A., Weller, P. J., Eds. *Handbook of Pharmaceutical Excipients*, 2nd ed.; American Pharmaceutical Association, The Pharmaceutical Press: 1994.
(9) Engström, S. *Lipid Technol.* **1990**, *2*, 42−45.
(10) Shah, J. C.; Sadhale, Y.; Murthy Chilukuri, D. *Adv. Drug Delivery Rev.* **2001**, *47*, 229−250.
(11) Landau, E. M.; Rosenbusch, J. P. *Proc. Natl. Acad. Sci. U.S.A.* **1996**, *93*, 14532−14535.
(12) Ridell, A.; Evertsson, H.; Nydén, M.; Engström, S., submitted for publication.
(13) Wulff, M.; Aldén, M.; Craig, D. Q. M. *Int. J. Pharm.* **1996**, *142*, 189−198.
(14) Aldén, M.; Lydén, M.; Tegenfeldt, J. *Int. J. Pharm.* **1994**, *110*, 267−276.
(15) Pielichowski, K.; Flejtuch, K. *Macromol. Mater. Eng.* **2003**, *288*, 259−264.
(16) Stribeck, N.; Alamo, R. G.; Mandelkern, L.; Zachmann, H. G. *Macromolecules* **1995**, *28*, 5029−5036.
(17) Huang, C.-I.; Chen, J.-R. *J. Polym. Sci., Part B: Polym. Phys.* **2001**, *39*, 3705−3715.
(18) Dreezen, G.; Koch, M. H. J.; Reynaers, H.; Groeninckx, G. *Polymer* **1999**, *4*, 6451−6463.
(19) Shieh, Y.-T.; Lin, Y.-G.; Chen, H.-L. *Polymer* **2002**, *43*, 3691−3698.
(20) Vonk, C. G.; Kortleve, G. *Kolloid Z. Z. Polym.* **1967**, *220*, 19−24.
(21) Ruland, W. *Colloid Polym. Sci.* **1977**, *255*, 417−427.
(22) Ruland, W. *J. Appl. Crystallogr.* **1971**, *4*, 70−73.
(23) Debye, P.; Anderson Jr., H. R.; Brumberger, H. *J. Appl. Phys.* **1957**, *28*, 679−683.
(24) Debye, P.; Bueche, A. M. *J. Appl. Phys.* **1949**, *20*, 518−525.
(25) Buckley, C. P.; Kovacs, A. J. *Colloid Polym. Sci.* **1976**, *254*, 695−715.
(26) Gaur, U.; Lau, S. F.; Shu, H. C.; Wunderlich, B. B. *J. Phys. Chem. Ref. Data* **1981**, *89*, 1001.
(27) Gaur, U.; Lau, S. F.; Shu, H. C.; Wunderlich, B. B. *J. Phys. Chem. Ref. Data* **1982**, *313*, 12.
(28) Gaur, U.; Lau, S. F.; Shu, H. C.; Wunderlich, B. B. *J. Phys. Chem. Ref. Data* **1983**, *29*, 91.
(29) Vidotto, G.; Lévy, D.; Kovacs, A. J. *J Kolloid Z. Z. Polym.* **1968**, *230*, 289−305.
(30) Varma-Nair, M.; Wunderlich, B. *J. Phys. Chem. Ref. Data* **1991**, *20*, 349.
(31) Malkin, T. *Prog. Chem. Fats Other Lipids* **1954**, *2*, 1−50.
(32) Larsson, K. *Ark. Kemi* **1965**, *23*, 35−56.
(33) Larsson, K. *Lipids—Molecular Organization, Physical Functions and Technical Applications*, 1st ed.; The Oily Press Ltd.: Dundee, Scotland, 1994; Vol. 5.
(34) Strobl, G. R.; Schneider, M. *J. Polym. Sci., Polym. Phys. Ed.* **1980**, *18*, 1343−1359.
(35) Santa Cruz, C.; Stribeck, N.; Zachmann, H. G.; Baltá Calleja, F. J. *Macromolecules* **1991**, *24*, 5980−5990.

MA0354344